Ion-Exchange Adsorption of Proteins: Experiments and Molecular Dynamics Simulations

Juan Liang[1,*], Georg Fieg[1], and Sven Jakobtorweihen[2]

DOI: 10.1002/cite.201400095

The adsorption of serum albumin and hemoglobin onto Q Sepharose FF was investigated, where the single and binary adsorption were considered. Both experiments and molecular dynamics simulations have been performed to study the adsorption from macroscopic and microscopic points of view. The steric mass-action model was applied to describe the single adsorption isotherms and to predict the binary isotherms. The results of the experiments and simulations were connected and compared by two parameters of the steric mass-action model. Both results present a preferential adsorption of serum albumin.

Keywords: Adsorption, Ion exchange, Protein

Received: July 01, 2014; *revised:* November 24, 2014; *accepted:* March 23, 2015

1 Introduction

Ion-exchange chromatography (IEC) has been extensively applied in protein purification [1, 2]. An understanding of ion-exchange adsorption plays a very important role in the development of this separation technology. At present, extensive IEC studies target the adsorption of single component proteins. The influence factors of ion-exchange adsorption have been widely investigated, including the types of proteins [3, 4], surface properties and structure characteristics of the adsorbent [5, 6], pH value [6 – 8], ionic strength [9] and system temperature [10].

In IEC applications, protein mixtures are loaded into an IEC column. The target protein competitively adsorbs onto the adsorbent. Therefore, a comprehensive understanding of both single- and multi-component adsorption is necessary for its improvement. In 1999, Lewus [11] studied the ion-exchange adsorption of mixtures of lysozyme and cytochrome c on S-HyperD-M. Competition between the two proteins was observed at high protein concentrations. In 2005, Cano [12] investigated the adsorption of cytochrome b_5 and α-lactalbumin mixtures. This was the first study of adsorption isotherms of binary protein mixtures. Zhou [13] analyzed the effect of the ionic strength on the binary adsorption isotherms. Aboudzadeh [14] studied the importance of protein sizes and the interactions among different proteins in binary adsorption. Xu [15] investigated the binary adsorption equilibrium under various conditions, where the results showed that the adsorption patterns largely follow the intrinsic protein-surface interaction, and the adsorption sequence does not affect the adsorption equilibrium. In summary, although the adsorption of binary proteins has been studied, more systematical analysis of the influencing factors and of the competition between different components in binary adsorption is needed. In particular, the effect of different adsorption sequences remains unclear.

For a better understanding of the protein adsorption and competition, both single and binary adsorption processes need to be explored further. Due to the lack of effective microscopic experimental techniques, molecular dynamics (MD) simulations [16] were used in this study to elucidate the details of the single and binary adsorption processes at the atomic level. MD simulations provide detailed microscopic information, and have been used to study the interactions in affinity chromatography [17]. Based on MD simulations, a mechanism model for the adsorption of lysozyme onto a SP Sepharose FF surface has been developed [18]. For a detailed description of protein behavior in hydrophobic charge induction chromatography, Zhang [19] modified a coarse-grained force field based on a statistical analysis. Moreover, MD simulations have been applied to investigate the protein conformational transitions within chromatographic pores [20, 21].

In this work, bovine/human serum albumin (BSA/HSA) and hemoglobin (bHb) were introduced as model proteins to investigate both single and binary adsorption onto Q Sepharpse FF. For a systematic understanding a comprehensive investigation combining experiments and MD simulations was performed. The well-known steric mass-action (SMA) model was chosen to describe the single adsorption isotherms and to predict the binary adsorption isotherms. The experimental and simulation results were quantitatively

[1]Dr.-Ing. Juan Liang (juan.liang@tu-harburg.de), Prof. Dr.-Ing. Georg Fieg, Hamburg University of Technology, Institute of Process and Plant Engineering, Schwarzenbergstraße 95, 21073 Hamburg, Germany; [2]Dr.-Ing. Sven Jakobtorweihen, Hamburg University of Technology, Institute of Thermal Separation Processes, Eissendorfer Straße 38, 21073 Hamburg, Germany.

compared. The results of this work are the basis for a better understanding of the ion-exchange adsorption of proteins, as well as for the design, optimization and control of ion-exchange chromatography.

2 Theoretical Model

The steric mass-action model [22] is widely used to describe protein ion-exchange adsorption. In the SMA model, protein adsorption on the ion-exchange adsorbent is treated as a stoichiometric reaction [23]. The multi-pointed nature of proteins and the steric hindrance of salt counterions are taken into account [22]. The SMA model for adsorption is given as:

$$c = \left(\frac{q}{K}\right)\left(\frac{c_s}{\Lambda - (\nu+\sigma)q}\right)^{\nu} \tag{1}$$

where K is the adsorption equilibrium constant, Λ is the total capacity of the adsorbent, ν is the characteristic charge equal to the amount of protein binding sites, σ is the steric factor of the protein, which is equal to the number of sterically hindered counterions, q is the protein concentration on the adsorbent (adsorption density), c is the protein concentration and c_s is the salt concentration in the liquid phase. For binary adsorption, the SMA model can be written as follows:

$$c_1 = \left(\frac{q_1}{K_1}\right)\left(\frac{c_s}{\Lambda - (\nu_1+\sigma_1)q_1 - (\nu_2+\sigma_2)q_2}\right)^{\nu_1} \tag{2a}$$

$$c_2 = \left(\frac{q_2}{K_2}\right)\left(\frac{c_s}{\Lambda - (\nu_1+\sigma_1)q_1 - (\nu_2+\sigma_2)q_2}\right)^{\nu_2} \tag{2b}$$

where the subscripts 1 and 2 refer to components 1 and 2, respectively.

In order to describe the accuracy of predictions with the SMA model, a residual sum of squares (RSS) error was introduced:

$$\mathrm{RSS} = \frac{\sum_{i=1}^{N}\left(\frac{q_{exp,i}+q_{cal,i}}{q_{exp,i}}\right)^2}{N} \tag{3}$$

where N is the number of experimental isotherm points, q_{exp} and q_{cal} are the experimental and calculated adsorption densities, respectively.

3 Methods

3.1 Experiments

Anion exchange adsorbent Q Sepharose FF was the purchased from GE Healthcare (Uppsala, Sweden). Both BSA (66.7 kD, pI = 4.9) and bHb (65.0 kD, pI = 7.0 – 7.4) were bought from Sigma-Aldrich (St. Louis, MO, USA).

Static adsorption experiments of pure proteins as well as binary mixtures were carried out at 298 K with the same procedure as described by Shi [24]. Both simultaneous and sequential binary experiments were performed to study the influence of the adsorption sequence on binary adsorption. 20 mmol L^{-1} phosphate buffers (pH 8.0, 9.0 with 0, 50, 100 mmol L^{-1} NaCl) were used. 0.1 g of drained Q Sepharose FF (overnight equilibrated) was mixed with 10 mL of protein solution. Thereafter, the mixture was kept in a water bath at a shaking speed of 150 rpm for 8 h to achieve equilibrium. After equilibrium was reached, the supernatant was collected. For single component experiments, the protein concentration c in the supernatant was determined with a UV/Vis spectrophotometer at 280 nm directly. In the binary experiments the absorbance of the total protein amount and bHb in the supernatant was measured at 280 and 360 nm, respectively. The adsorption densities were calculated from a mass balance.

The sequential adsorption was conducted only at pH 8.0 in two steps. First, pre-adsorption of pure BSA (c_0) was performed as described above to achieve equilibrium. After the equilibrium, the supernatant was removed. The concentration at equilibrium in the liquid phase c_{pre} and the adsorption density of BSA q_{pre} were obtained. Then, the BSA-bounded adsorbent was mixed with 10 mL mixture of BSA and bHb, in which initial liquid phase concentrations of bHb and BSA were equal to c_0 and c_{pre}, respectively. After shaking in a water bath for 8 h, the supernatant was collected and the final concentrations of BSA and bHb were measured. The adsorption densities of bHb and BSA were calculated from mass balance. The adsorption density for BSA in the whole sequential adsorption (sum of its adsorption densities in the two described steps) will be reported in Sect. 4.3.

3.2 Simulation Details

The simulations were carried out with the simulation package GROMACS 4.5 [25]. Considering the large size of the ion-exchange systems, the MARTINI coarse-grained (CG) force field [26 – 28] was applied. These simulations were carried out for pH 7.0, c_s = 230 mmol L^{-1}. The ion-exchange system contains proteins, ligands (with quaternary amine group) and the chromatographic base. At the bottom of the simulation box (19.604 nm x 20.404 nm x 20 nm), the chromatographic matrix was set as a smooth plate defined as P_4 particles. 1116 ligands were put on top of the wall as a uniform layer with the roots restrained to mimic the immobilization (see Fig. 1). The CG model of ligands was modeled with three MARTINI particles (P_4-P_4-Q_0), test shows the applicability of this model (results not shown). One or two protein molecules were placed in the liquid phase. The CG models of the proteins were generated according to the pro-

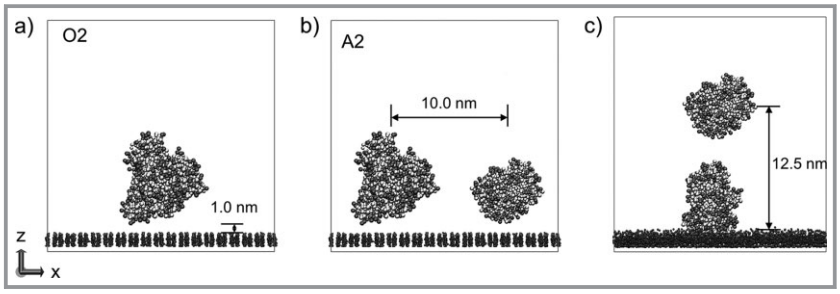

Figure 1. Initial configurations of the simulations: a) single adsorption of HSA (here set-up O2 is shown); b) simultaneous adsorption of HSA and bHb (here set-up A2 is shown); c) sequential adsorption of HSA and bHb.

tein mapping principle of the MARTINI force field [28], starting from their atomistic structures from the Protein Data Bank (HSA, PDB ID 1AO6 (chain A); bHb, PDB ID 1G0A).

BSA is a one of the commonest model proteins studied in experiments. For better comparison and combination with the results of other researches, BSA was used in the experimental part of this work. Unfortunately, the crystal structure of BSA is still unclear. Therefore, HSA rather than BSA was studied in the simulations. The justification of using HSA and BSA for serum albumin is given by their great sequence homologies [29], similar structures [30] and identical adsorption behavior [7]. In single component simulations the protein was placed with a minimum distance to the ligands of 1.0 nm (see Fig. 1a). For each protein, six different initial orientations (with 90° rotation difference) were simulated [19]. The six orientations will be represented in this work as O1-O6. In simultaneous binary simulations both proteins were initially placed next to each other with a minimum distance to the ligands of 1.0 nm. The distance between the centers of mass of the proteins was set to be 10.0 nm (see Fig. 1b). Four different arrangements of HSA-bHb were investigated as behind-front (A1), left-right (A2), front-behind (A3) and right-left (A4). These differ by the protein sides facing each other. In the sequential simulation, HSA was pre-adsorbed, taken from the end of the single adsorption simulation named O2. bHb was put on top of this HSA, with the center of mass 12.5 nm away from the ligands (see Fig. 1c). The simulation box was further filled with water and ion particles. The standard CG water (P_4) in the MARTINI force field was used [27]. To avoid the freezing problem of the MARTINI water, 10 % of the standard water particles were replaced by a special type of particles called antifreeze particles (BP_4), this setup was reported to model the water successfully in simulations with the MARTINI force field [31]. A cation and an anion are modeled as Q_d and Q_a particles, respectively [27].

The basic parameters of the simulations were used as suggested in previous studies employing the MARTINI force field [26, 28, 32]. Since long-range interactions are important in ion-exchange systems, reaction field [33] was used herein to calculate the long-range electrostatic interactions. However, reaction field is not the perfect method for heterogeneous systems, but it is faster than Ewald method and, therefore, used for the large systems studied in this work. Initially, all systems have been energy-minimized. All simulations contained two parts: (1) 100 ns equilibration of chromatographic media, where the positions of the protein particles were restrained; (2) adsorption simulations with unrestrained proteins. The MD simulations were analyzed by the GROMACS suite of programs. Only results of the second part are presented and discussed.

4 Results and Discussion

4.1 Single-Component Adsorption

Single-component adsorption equilibria of BSA and bHb on Q Sepharose FF at pH 8.0 and 9.0 are shown in Fig. 2.

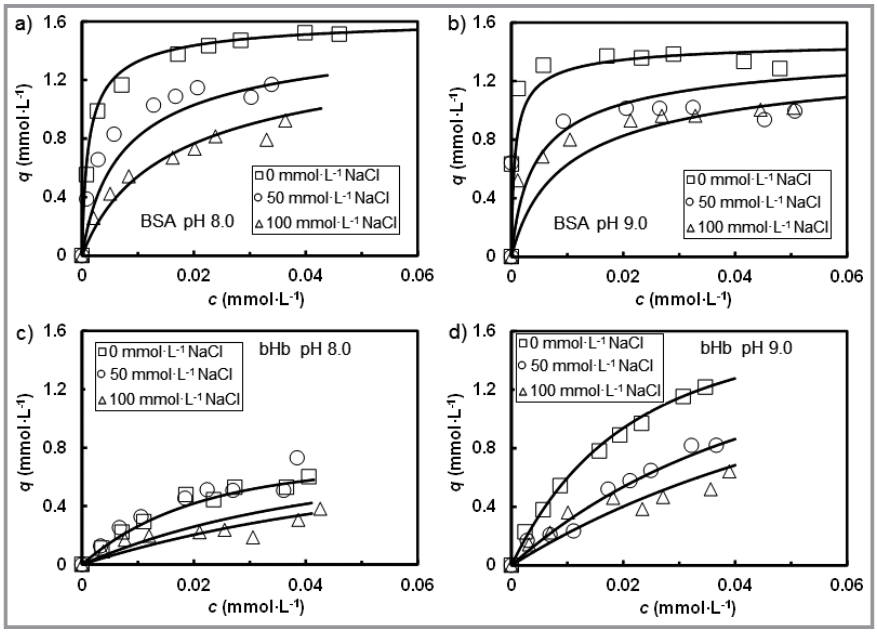

Figure 2. Single adsorption isotherms of BSA (a, b) and bHb (c, d) at pH 8.0 (a, c) and pH 9.0 (b, d). The lines are calculated isotherms using of the SMA model (for SMA parameters see Tab. 1).

BSA has a higher adsorption density than bHb at both pH values. The reason is that BSA has stronger electrostatic interaction with the adsorbent due to its higher negative charge at the studied pH values. As the buffer pH increases, the adsorption densities of both proteins increase due to an increase in their negative charge. The adsorption density of bHb increases at all protein concentrations, while that of BSA increases at low protein concentrations only. The reason is that the saturation of adsorbent was already reached at high concentrations of BSA. Moreover, an increase in salt concentration leads to a decrease of adsorption densities for both proteins under most conditions. This tendency is attributed to the well-known electrostatic screening effect [24, 34], which leads to a weaker protein-surface interaction at high salt concentrations. Two exceptions (BSA from 50 to 100 mmol L^{-1} NaCl at pH 9.0, bHb from 0 to 50 mmol L^{-1} NaCl at pH 8.0) indicate the complexity of the ion-exchange adsorption of proteins. The protein-surface interaction could partially be superimposed by protein-protein interaction, especially in adsorption associated with weak protein-surface interactions.

In Fig. 2 the fitted isotherms of the SMA model are shown. The single-component parameters of the SMA model obtained by fitting the experimental isotherms are listed in Tab. 1. The total ion-exchange capacity of the anion-exchange adsorbent (Λ) was determined to be 274.7 mmol L^{-1}. As Tab. 1 shows, the parameters ν and K of BSA are larger than those of bHb under all conditions. This further confirms the stronger adsorption of BSA. The σ values of BSA and bHb at pH 9.0 are similar, due to the similar sizes of these two proteins, while bHb has a much larger σ of 373 at pH 8.0 due to its weak interaction with the adsorbent. The value of K of both proteins increases with an increasing of pH due to more negatively charged proteins and stronger interaction at higher pH. Only a slight increase of ν can be seen for both proteins when the pH increases.

The single-component systems were simulated for 400 ns. During these simulations, the protein moved to the ligands and adsorbed due to attractive protein-ligand interactions. The simulation results present the influences of the initial protein orientation on the protein adsorption. Both protein-ligand potential energies and protein-ligand minimum distances have been calculated and analyzed to investigate the adsorption [32]. Stable low values of interaction energies and minimum distances indicate a stable adsorption. It is evident that HSA reached a stable adsorption from all six different orientations, while bHb was adsorbed only from O2. These simulation results are qualitatively consistent with the experimental results.

Two parameters (ν and σ) of the SMA model which have a physical basis were determined from the MD simulations (shown in Tab. 1). The last 10 ns of each trajectory were analyzed to calculate the binding sites and the hindered ligands/counterions. The protein residues having a minimum ligand distance smaller than 0.45 nm were considered as binding sites. The exchange groups of the ligands with a minimum distance to the protein between 0.45 nm and 2.5 nm were considered as sterically hindered ligands/counterions. The values of each orientation were averaged over time, and the average values over the six orientations are shown in Tab. 1. HSA has 1 – 3 binding sites in the adsorbed states from different initial orientations. bHb has only one binding site in case a stable adsorption is reached (orientation O2). All binding sites of both proteins are negatively charged residues. This indicates that the main driving forces for the adsorption are electrostatic interactions. Most of the characteristic charges and the steric factors of HSA and bHb are consistent with the experimental values (see Tab. 1). Only the steric factor of bHb at pH 8 determined in experiments is much larger. The difference in pH between the experiments and the simulations could be a reason for this deviation. However, the comparison confirms that the MD simulations are capable to model the protein adsorption onto ion-exchange adsorbent with electrostatic interactions as driving force. More information on the single-component simulation can be found in [32].

4.2 Simultaneous Binary Adsorption

For binary adsorption the initial concentration ratio (BSA:bHb) was set to be 1:1. The corresponding isotherms of both BSA and bHb are shown in Fig. 3. BSA still shows a higher adsorption density than bHb at both pH values. Moreover, by comparing Fig. 2 and 3, it can be seen that the adsorption densities of both proteins decrease in binary adsorption. The proteins adsorb competitively onto the ion-exchange chromatographic media, and BSA adsorbed preferentially. As presented in Fig. 3 (a, b), the increase of pH and the decrease of salt concentration result in higher adsorption densities of BSA. The pH and ionic strength of the buffer have an influence on BSA adsorption. On the

Table 1. Parameters of the SMA model for BSA/HSA and bHb in single-component adsorption.

		BSA/HSA			bHb		
		ν	K	σ	ν	K	σ
Experiment	pH 8.0	1.56	27.70	164	0.57	7.65	373
	pH 9.0	1.64	39.72	182	0.67	13.82	160
Simulation [32]		1.8 ± 0.7	–	177.0 ± 23.7	0.6 ± 0.5	–	133.0 ± 67.0

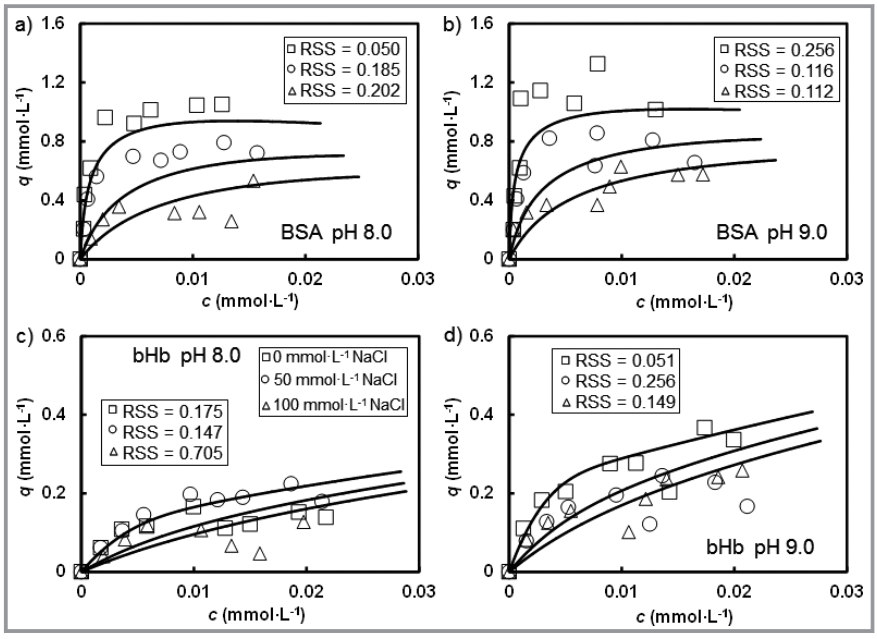

Figure 3. Simultaneous binary adsorption isotherms of BSA (a, b) and bHb (c, d) at pH 8.0 (a, c) and pH 9.0 (b, d). The lines are calculated isotherms using of the SMA model (see Tab. 1 for the parameters). RSS values for the predicted isotherms are shown.

contrary, the adsorption of bHb was mainly influenced by the competitor BSA rather than by the buffer constituents (see Fig. 3 (c, d)). The SMA model with parameters obtained from single adsorption (shown in Tab. 1) has been used for the prediction (lines in Fig. 3). The results show that the SMA model can predict the binary isotherms qualitatively. However, quantitative deviations can be seen (RSS values in Fig. 3), especially at higher initial concentrations. For a better analysis of whether the parameters of single adsorption could be directly used in binary predictions, the MD simulation results of simultaneous adsorption will be discussed.

In order to study the binary competitive adsorption in detail, the simultaneous binary adsorption has been simulated for 600 ns. The results of the simulations of four different arrangements show that HSA adsorbs from all these four arrangements, while bHb adsorbs only from A1 and A2. An interaction between HSA and bHb was observed in all these simulations, which indicates the competition between different components. Two parameters (ν and σ) of the SMA model were determined directly by the MD simulations. The results shown in Tab. 2 are the average values of each protein from all four arrangements. It can be seen that the values of these two parameters for both proteins in single and binary MD simulations are consistent. Hence, the SMA parameters of single adsorption could be used directly to predict binary adsorption. Considering the results of the binary simulations, the deviations of the predicted binary isotherms (shown in Fig. 2) were probably due to the lack of a parameter describing the interaction and competition between different components.

4.3 Sequential Binary Adsorption

The adsorption densities of BSA and bHb as well as the total adsorption density (sum of both proteins) from sequential adsorption experiments are shown in Fig. 4. Two triangles representing the total adsorption densities overlap at $c = 0.078\ \mathrm{mmol\,L^{-1}}$ (see Fig. 4). Due to the multistep adsorption process and the indirect measurement of the adsorption densities for BSA, the accuracy of the isotherms in sequential adsorption is lowered. As can be seen in Fig. 4, after the pre-adsorption of BSA, the decrease of adsorption density of BSA in the second step indicates a displacement by bHb, especially at high

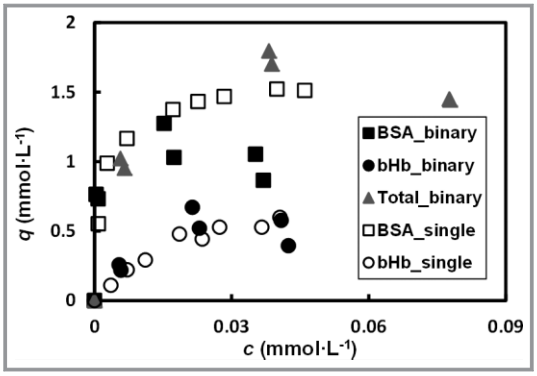

Figure 4. Adsorption isotherms of BSA and bHb in single and sequential binary adsorption, and total protein density in sequential binary adsorption.

Table 2. Parameters of the SMA model for HSA and bHb obtained from MD simulations.

	HSA		bHb	
	ν	σ	ν	σ
Simultaneous binary adsorption	2.6 ± 1.0	182.0 ± 22.0	0.6 ± 0.4	136.6 ± 44.3
Single component (O2) adsorption	3.0	192.3	0.9	158.8

concentrations. The adsorption densities of bHb in sequential adsorption were pretty much the same as in its single adsorption. These discrepancies suggest the influence of the adsorption sequence in binary adsorption.

Instead of a decrease in total adsorption densities due to the competition in binary adsorption, higher total adsorption densities in sequential adsorption than those in single adsorption can be obviously seen in Fig. 4. A possible reason is that bHb adsorbed on the pre-adsorbed BSA. A similar phenomenon was also reported in bHb adsorption on hydrophobic surface by Hook [35]. The multiple layer adsorption of bHb was further investigated by MD simulations on a molecular scale. The sequential adsorption has been simulated for 2000 ns. The minimum protein-protein and protein-ligand distances are shown in Fig. 5. It can be seen that bHb moves to the pre-adsorbed HSA and adsorbs onto it around 630 ns. Afterwards, bHb keeps fluctuating with a distance of about 2.0 nm to the ligands and gets quite close to the ligands at approx. 1650 ns. Here, it can be concluded that if the ion-exchange adsorbent is saturated with HSA, bHb can then adsorb onto HAS due to the lack of available ligands without a further contact with the ligands. The multiple layer adsorption of bHb onto adsorbed proteins is seen in both experiments and simulations.

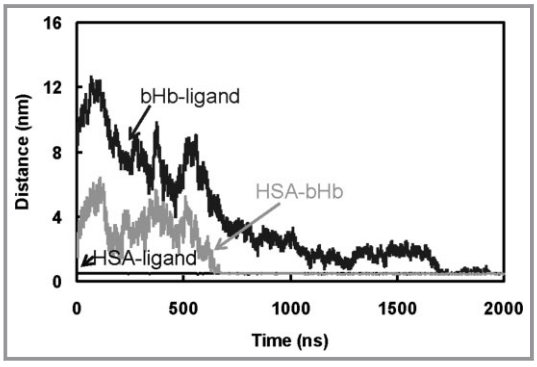

Figure 5. Minimum distance between HSA and the ligands, between bHb and the ligands, and between HSA and bHb in a sequential adsorption simulation.

5 Conclusions

Serum albumin and hemoglobin were used to investigate the adsorption of single and binary protein mixtures onto Q Sepharose FF. A comprehensive investigation combining experiments and MD simulations was performed. The results of the experiments and the simulations were compared quantitatively by two parameters of the SMA model. The MD simulations with a coarse-grained model have been successfully used to investigate ion-exchange adsorption processes. Both experimental and simulation results show that serum albumin adsorbed stronger than hemoglobin. The two proteins adsorbed competitively onto the adsorbent in binary adsorption. In binary adsorption, the buffer condition had influence on serum albumin but almost no influence on hemoglobin. The adsorption sequence affects the binary adsorption. The multiple layer adsorption of hemoglobin in sequential adsorption was observed in the experiments and was further discussed with the MD simulations. The SMA model with parameters obtained from single adsorption can be directly used to predict the binary adsorption qualitatively. For a further modification, parameters describing interaction and competition between different components should be added to the multi-component model.

This work was supported by the China Scholarship Council.

Symbols used

c	[mmol L^{-1}]	protein concentration in liquid phase
c_s	[mmol L^{-1}]	salt concentration
K	[–]	adsorption equilibrium constant
q	[mmol L^{-1}]	adsorption density
ν	[–]	characteristic charge
Λ	[–]	total capacity of the adsorbent
σ	[–]	steric factor

References

[1] S. R. Himmelhoch, *Method. Enzymol.* **1971**, *22*, 273 – 286. DOI: 10.1016/0076-6879(71)22028-0
[2] Q. Z. Qin, J. J. Mao, Z. H. Jin, *Chemical separation methods*, Atomic Energy, Beijing **1984**.
[3] A. K. Hunter, G. Carta, *J. Chromatogr. A* **2002**, *971*, 105 – 116. DOI: 10.1016/S0021-9673(02)01027-0
[4] Y. Yuan, M. R. Oberholzer, A. M. Lenhoff, *Colloid. Surface. A* **2000**, *165 (1 – 3)*, 125 – 141. DOI: 10.1016/S0927-7757(99)00418-5
[5] J. R. Conder, B. O. Hayek, *Biochem. Eng. J.* **2000**, *6 (3)*, 225 – 232. DOI: 10.1016/S1369-703X(00)00094-2
[6] A. Katiyar, L. Ji, P. Smirniotis, N. G. Pinto, *J. Chromatogr. A* **2005**, *1069 (1)*, 119 – 126. DOI: 10.1016/j.chroma.2004.10.077
[7] J. C. Bosma, J. A. Wesselingh, *AIChE J.* **1998**, *44 (11)*, 2399 – 2409. DOI: 10.1002/aic.690441108
[8] Z. G. Peng, K. Hidajat, M. S. Uddin, *J. Colloid. Interf. Sci.* **2004**, *271 (2)*, 277 – 283. DOI: 10.1016/j.jcis.2003.12.022
[9] S. P. Zhang, Y. Sun, *AIChE J.* **2002**, *48 (1)*, 178 – 186. DOI: 10.1002/aic.690480118
[10] R. Janzen, K. K. Unger, W. Muller, M. T. W. Hearn, *J. Chromatogr.* **1990**, *522*, 77 – 93. DOI: 10.1016/0021-9673(90)85179-Y
[11] R. K. Lewus, G. Carta, *AIChE J.* **1999**, *45 (3)*, 512 – 522. DOI: 10.1002/aic.690450308
[12] T. Cano, N. D. Offringa, R. C. Willson, *J. Chromatogr. A* **2005**, *1079 (1 – 2)*, 116 – 126. DOI: 10.1016/j.chroma.2005.03.120
[13] X. P. Zhou, X. L. Su, Y. Sun, *Biotechnol. Progr.* **2007**, *23 (5)*, 1118 – 1123. DOI: 10.1021/bp070092x
[14] M. R. Aboudzadeh, N. Aboudzadeh, J. W. Zhu, B. Wu, *Korean J. Chem. Eng.* **2007**, *24 (4)*, 641 – 647. DOI: 10.1007/s11814-007-0017-7

[15] X. K. Xu, A. M. Lenhoff, *J. Chromatogr. A* **2009**, *1216 (34)*, 6177 – 6195. DOI: 10.1016/j.chroma.2009.06.082
[16] D. Frenkel, B. Smit, *Understanding Molecular Simulation: From Algorithms to Applications*, 2nd ed., Computational Science Series Academic Press, San Diego **2002**.
[17] L. Zamolo, V. Busini, D. Moiani, D. Moscatelli, C. Cavallotti, *Biotechnol. Progr.* **2008**, *24 (3)*, 527 – 539. DOI: 10.1021/bp070469z
[18] F. Dismer, J. Hubbuch, *J. Chromatogr. A* **2010**, *1217 (8)*, 1343 – 1353. DOI: 10.1016/j.chroma.2009.12.061
[19] L. Zhang, S. Bai, Y. Sun, *J. Mol. Graph. Model.* **2011**, *29 (7)*, 906 – 914. DOI: 10.1016/j.jmgm.2011.02.004
[20] L. Zhang, G. F. Zhao, Y. Sun, *J. Phys. Chem. B* **2009**, *113 (19)*, 6873 – 6880. DOI: 10.1021/jp809754k
[21] L. Zhang, D. N. Lu, Z. Liu, *J. Chromatogr. A* **2009**, *1216 (12)*, 2483 – 2490. DOI: 10.1016/j.chroma.2009.01.038
[22] C. A. Brooks, S. M. Cramer, *AIChE J.* **1992**, *38 (12)*, 1969 – 1978. DOI: 10.1002/aic.690381212
[23] V. Noinville, C. Vidalmadjar, B. Sebille, *J. Phys. Chem.* **1995**, *99 (5)*, 1516 – 1522. DOI: 10.1021/j100005a023
[24] Q. H. Shi, Z. Cheng, Y. Sun, *J. Chromatogr. A* **2009**, *1216 (33)*, 6081 – 6087. DOI: 10.1016/j.chroma.2009.06.065
[25] B. Hess, C. Kutzner, D. van der Spoel, E. Lindahl, *J. Chem. Theory Comput.* **2008**, *4 (3)*, 435 – 447. DOI: 10.1021/ct700301q
[26] S. J. Marrink, H. J. Risselada, S. Yefimov, D. P. Tieleman, A. H. de Vries, *J. Phys. Chem. B* **2007**, *111 (27)*, 7812 – 7824. DOI: 10.1021/jp071097f
[27] S. J. Marrink, A. H. de Vries, A. E. Mark, *J. Phys. Chem. B* **2004**, *108 (2)*, 750 – 760. DOI: 10.1021/jp036508g
[28] L. Monticelli, S. K. Kandasamy, X. Periole, R. G. Larson, D. P. Tieleman, S. J. Marrink, *J. Chem. Theory Comput.* **2008**, *4 (5)*, 819 – 834. DOI: 10.1021/ct700324x
[29] T. Peters, *Adv. Protein Chem.* **1985**, *37*, 161 – 245.
[30] A. Michnik, *J. Therm. Anal. Calorim.* **2003**, *71 (2)*, 509 – 519. DOI: 10.1023/A:1022851809481
[31] S. J. Marrink, H. J. Risselada, S. Yefimov, D. P. Tieleman, A. H. de Vries, *J. Phys. Chem.* **2007**, *111 (27)*, 7812 – 7824. DOI: 10.1021/jp071097f
[32] J. Liang, G. Fieg, F. J. Keil, S. Jakobtorweihen, *Ing. Eng. Chem. Res.* **2012**, *51 (49)*, 16049 – 16058. DOI: 10.1021/ie301407b
[33] I. G. Tironi, R. Sperb, P. E. Smith, W. F. Vangunsteren, *J. Chem. Phys.* **1995**, *102 (13)*, 5451 – 5459. DOI: 10.1063/1.469273
[34] Q. H. Shi, Y. Zhou, Y. Sun, *Biotechnol. Progr.* **2005**, *21 (2)*, 516 – 523. DOI: 10.1021/bp049735o
[35] F. Hook, M. Rodahl, B. Kasemo, P. Brzezinski, *P. Natl. Acad. Sci. USA.* **1998**, *95 (21)*, 12271 – 12276.

